Component	Fit into the tomographic map	Localization	Orientation
Nup107-NTD/ Nup96/ Sec13	inner stem base NR outer stem base NR 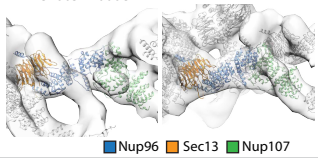 Nup96 Sec13 Nup107	Location: unambiguous • restrained by known interactors within the Y-complex [1, 2, 3, 4] • consistent with C2 symmetric localization to CR and NR [5, 6, 7] • consistent with measured stoichiometry [8] 	Orientation: unambiguous • consistent with known orientation within larger vertex structure [1,9] • identified by systematic fitting with very high confidence (Ext. Data Fig. 7) • pronounced intrinsic asymmetry of template structure (Ext. Data Tab. 1)
Nup160/ Nup37	inner large arm CR outer large arm CR 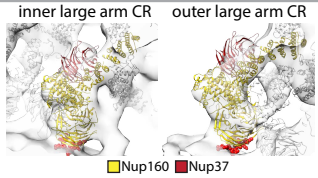 Nup160 Nup37 *Predicted membrane binding motif marked in red*	Location: unambiguous • restrained by known interactors within the Y-complex [1, 2, 3, 4] • consistent with C2 symmetric localization to CR and NR [6, 7] • consistent with measured stoichiometry [8] 	Orientation: unambiguous • consistent with known orientation within larger vertex structure [1,9] • identified by systematic fitting with very high confidence • pronounced intrinsic asymmetry of template structure (Ext. Data Tab. 1) • consistent with predicted membrane binding motif [10] (Ext. Data Fig. 6b)
Nup85-NTD/ Seh1		Location: unambiguous • restrained by known interactors within the Y-complex [1, 2, 3, 4] • consistent with C2 symmetric localization to CR and NR [6, 7] • consistent with measured stoichiometry [8] 	Orientation: unambiguous • consistent with known orientation within larger vertex structure [1,9] • identified by systematic fitting with very high confidence • pronounced intrinsic asymmetry of template structure (Ext. Data Tab. 1)
Nup85-CTD	inner small arm NR outer small arm NR Nup85-NTD 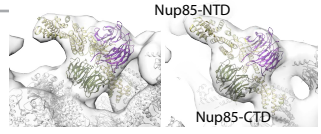 Nup85-CTD Nup43 Nup85 Seh1	Location: unambiguous • restrained by known interactors within the Y-complex [1, 2, 3, 4] • consistent with C2 symmetric localization to CR and NR [6, 7] • consistent with measured stoichiometry [8]	Orientation: partially restrained • consistent with known orientation within larger vertex structure [1,9] but may rotate around long axis of the fold • Homology model extending Nup85-NTD. The model has low confidence in exact helix positioning
Nup43	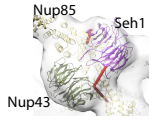 Nup85 Seh1 Nup43	Location: unambiguous • restrained by known interactors within the Y-complex [1, 11] • consistent with C2 symmetric localization to CR and NR [6, 7] • consistent with measured stoichiometry [8] 	Orientation: unambiguous • restrainted by cross-linking MS data [1] • consistent with local refinment using Haddock without restraints (see Methods)
Nup107-CTD/ Nup133-CTD	inner stem tip NR outer stem tip NR 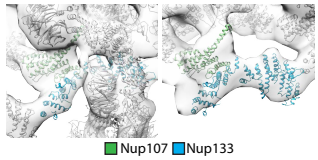 Nup107 Nup133	Location: unambiguous • restrained by known interactors within the Y-complex [1, 2, 3, 4] • consistent with C2 symmetric localization to CR and NR [5, 6, 7] • consistent with measured stoichiometry [8] 	Orientation: unambiguous • consistent known connectivity to vertex and Nup133 structure [1,9] • consistent with systematic fitting • pronounced intrinsic asymmetry of template structure (Ext. Data Tab. 1) 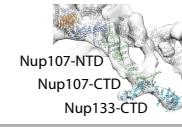 Nup107-NTD Nup107-CTD Nup133-CTD
Nup133-NTD	inner stem tip NR outer stem tip NR 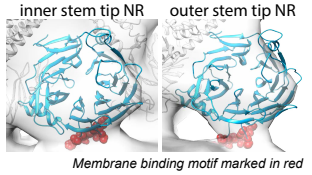 *Membrane binding motif marked in red*	Location: unambiguous • restrained by known interactors within the Y-complex [1, 2, 3, 4] and head to tail contact to Nup160 [12, 13] • consistent with C2 symmetric localization to CR and NR [6, 7] • consistent with measured stoichiometry [8] 	Orientation: partially restrained • although restrained by its known membrane binding motif [10] (Ext. Data Fig. 6b), the beta propellor might flip by 180 degree around an axis paralell to the nucleocytoplasmic transport axis. The orientation shown would be consistent with its connectivity to the Nup133-CTD (Ext. Data Fig. 6b) but the domain linker is flexible.
Elys-NTD	inner outer 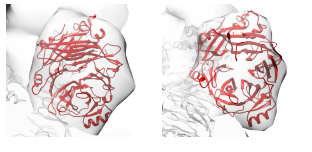	Location: unambiguous • restrained by known interactors within the Y-complex [1, 3, 14] • consistent with asymmetric localization to NR [6, 15] and additional density observed in the tomographic map • consistent with measured stoichiometry [8] 	Orientation: partially restrained • restrained only by the local asymmetry of the tomographic density that is highly consistent with the shape of the high resolution structure. A 180 degree flip of the structure around an axis parallel to the NE might be possible.

Component	Fit into the tomographic map	Localization	Orientation
Nup155-NTD/ Nup155-CTD	connector between IR and CR/NR 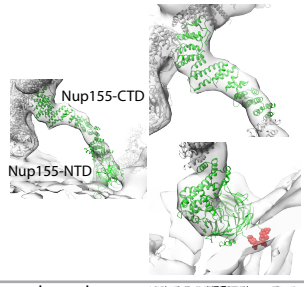 *Membrane binding motif marked in red*	**Location: unambiguous** • consistent with proximity to membrane, possibly transmembrane domain [16] (Ext. Data Fig. 1a) and Nup155 CTD • consistent with C2 symmetric localization to IR [6] • NTD identified by systematic fitting with very high confidence (Ext. Data Fig. 7); extension with CTD is highly consitent with tomographic density • consistent with observed weak interactions to CR and/or NR members (e.g. Nup214 and Sec13, Ext. Data Fig. 8)	**Orientation: unambiguous** • NTD identified by systematic fitting with very high confidence (Ext. Data Fig. 7); extension with CTD is highly consistent with tomographic density • pronounced intrinsic asymmetry of template structure (Ext. Data Tab. 1) • consistent with experimetally determined membrane binding motif (Fig. 3b, d)
Nup155-NTD/ Nup155-CTD	inner ring 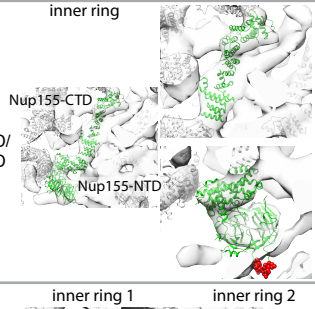 *Membrane binding motif marked in red*	**Location: suggestive** • suggestive assignment because of limited structural and biochemical information available for the IR members • consistent with proximity to membrane, and possibly transmembrane domain [16] (Ext. Data Fig. 1a) and Nup155 CTD • consistent with C2 symmetric localization to IR [6] • NTD identified by systematic fitting with very high confidence (Ext. Data Fig. 7); extension with CTD highly consistent with tomographic density	**Orientation: unambiguous** • if suggestive position is correct, the tomographic density would not permit an alternative orientation because of the pronounced intrinsic asymmetry of template structure (Ext. Data Tab. 1) • NTD identified by systematic fitting with very high confidence (Ext. Data Fig. 7); extension wuth CTD highly consistent with tomographic density • consistent with experimetally determined membrane binding motif (Fig. 3b, d)
Nup205-NTD	inner ring 1 inner ring 2 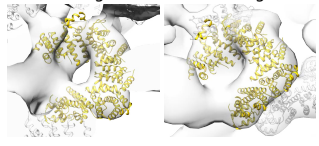	**Location: suggestive** • suggestive assignment because of limited structural and biochemical information available for the IR members • structurally homologous to Nup188 [18] that might substitute this position • consistent with C2 symmetric localization [5, 6] • NTD identified by systematic fitting with very high confidence (Ext. Data Fig. 7); • extension with CTD consistent with question mark-shape observed in isolation [17] • consistent with measured stoichiometry [8]	**Orientation: partially restrained** • might be flipped around an axis paralell to the NE plane • identified by systematic fitting with very high confidence (Ext. Data Fig. 7) inner ring 1 inner ring 2 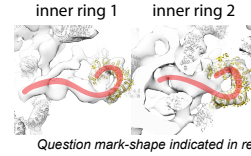 *Question mark-shape indicated in red*
Nup188-NTD	NR 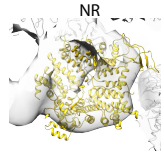	**Location: suggestive** • suggestive assignment because of limited structural and biochemical information available for the IR members • structurally homologous to Nup205 [18] that might substitute this position • consistent with biochemical data (Fig. 3, Ext. Data Fig. 8), cross-linking MS data [1], FRET data [19] • NTD identified by systematic fitting with very high confidence (Ext. Data Fig. 7); • extension with CTD consistent with question mark-shape observed in isolation [17] • consistent with measured stoichiometry [8]	**Orientation: partially restrained** • might be flipped around an axis paralell to the NE plane • identified by systematic fitting with very high confidence (Ext. Data Fig. 7) NR 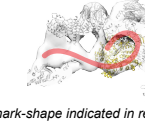 *Question mark-shape indicated in red*

1 Bui, K. H. et al. Integrated structural analysis of the human nuclear pore complex scaffold. Cell 155, 1233-1243, doi:10.1016/j.cell.2013.10.055 (2013).

2 Shi, Y. *et al.* Structural characterization by cross-linking reveals the detailed architecture of a coatomer-related heptameric module from the nuclear pore complex. *Mol Cell Proteomics* **13**, 2927-2943, doi:10.1074/mcp.M114.041673 (2014).

3 Thierbach, K. *et al.* Protein interfaces of the conserved Nup84 complex from Chaetomium thermophilum shown by crosslinking mass spectrometry and electron microscopy. *Structure* **21**, 1672-1682, doi:10.1016/j.str.2013.07.004 (2013).

4 Kampmann, M. & Blobel, G. Three-dimensional structure and flexibility of a membrane-coating module of the nuclear pore complex. *Nature Structural & Molecular Biology* **16**, 782-788, doi:nsmb.1618 [pii] 10.1038/nsmb.1618 (2009).

5 Krull, S., Thyberg, J., Bjorkroth, B., Rackwitz, H. R. & Cordes, V. C. Nucleoporins as components of the nuclear pore complex core structure and Tpr as the architectural element of the nuclear basket. *Mol Biol Cell* **15**, 4261-4277, doi:10.1091/mbc.E04-03-0165 (2004).

6 Rout, M. P. *et al.* The yeast nuclear pore complex: composition, architecture, and transport mechanism. *Journal of Cell Biology* **148**, 635-651 (2000).

7 Szymborska, A. *et al.* Nuclear pore scaffold structure analyzed by super-resolution microscopy and particle averaging. *Science* **341**, 655-658, doi:10.1126/science.1240672 (2013).

8 Ori, A. *et al.* Cell type-specific nuclear pores: a case in point for context-dependent stoichiometry of molecular machines. *Mol Syst Biol* **9**, 648, doi:msb20134 [pii] 10.1038/msb.2013.4 (2013).

9 Stuwe, T. *et al.* Nuclear pores. Architecture of the nuclear pore complex coat. *Science* **347**, 1148-1152, doi:10.1126/science.aaa4136 (2015).

10 Drin, G. *et al.* A general amphipathic alpha-helical motif for sensing membrane curvature. *Nat Struct Mol Biol* **14**, 138-146, doi:10.1038/nsmb1194 (2007).

11 Kim, D. I. *et al.* Probing nuclear pore complex architecture with proximity-dependent biotinylation. *Proc Natl Acad Sci U S A* **111**, E2453-2461, doi:10.1073/pnas.1406459111 (2014).

12 Alber, F. *et al.* The molecular architecture of the nuclear pore complex. *Nature* **450**, 695-701, doi:nature06405 [pii] 10.1038/nature06405 (2007).

13 Seo, H. S. *et al.* Structural and functional analysis of Nup120 suggests ring formation of the Nup84 complex. *Proc Natl Acad Sci U S A* **106**, 14281-14286, doi:10.1073/pnas.0907453106 (2009).

14 Bilokapic, S. & Schwartz, T. U. Molecular basis for Nup37 and ELY5/ELYS recruitment to the nuclear pore complex. *Proc Natl Acad Sci U S A* **109**, 15241-15246, doi:1205151109 [pii] 10.1073/pnas.1205151109 (2012).

15 Rasala, B. A., Orjalo, A. V., Shen, Z. X., Briggs, S. & Forbes, D. J. ELYS is a dual nucleoporin/kinetochore protein required for nuclear pore assembly and proper cell division. *Proceedings of the National Academy of Sciences, USA* **103**, 17801-17806, doi:Doi 10.1073/Pnas.0608484103 (2006).

16 Eisenhardt, N., Redolfi, J. & Antonin, W. Interaction of Nup53 with Ndc1 and Nup155 is required for nuclear pore complex assembly. *J Cell Sci* **127**, 908-921, doi:10.1242/jcs.141739 (2014).

17 Flemming, D. *et al.* Analysis of the yeast nucleoporin Nup188 reveals a conserved S-like structure with similarity to karyopherins. *J Struct Biol* **177**, 99-105, doi:S1047-8477(11)00323-6 [pii] 10.1016/j.jsb.2011.11.008 (2012).

18 Andersen, K. R. *et al.* Scaffold nucleoporins Nup188 and Nup192 share structural and functional properties with nuclear transport receptors. *eLife* **2**, e00745, doi:10.7554/eLife.00745 (2013).

19 Damelin, M. & Silver, P. A. In situ analysis of spatial relationships between proteins of the nuclear pore complex. *Biophysical journal* **83**, 3626-3636, doi:10.1016/S0006-3495(02)75363-0 (2002).